

## Annealing effect on the optical response and interdiffusion of n-ZnO/p-Si (111) heterojunction grown by atomic layer deposition

Ching-Shun Ku, Jheng-Ming Huang, Ching-Yuan Cheng, Chih-Ming Lin, and Hsin-Yi Lee

Citation: *Applied Physics Letters* **97**, 181915 (2010); doi: 10.1063/1.3511284

View online: <http://dx.doi.org/10.1063/1.3511284>

View Table of Contents: <http://scitation.aip.org/content/aip/journal/apl/97/18?ver=pdfcov>

Published by the *AIP Publishing*

---

### Articles you may be interested in

[Improved optical properties of ZnO thin films by concurrently introduced interfacial voids during thermal annealing](#)

*Appl. Phys. Lett.* **99**, 023105 (2011); 10.1063/1.3609321

[Structural characteristics of ZnO films grown on \(0001\) or \(11-20\) sapphire substrates by atomic layer deposition](#)

*J. Vac. Sci. Technol. A* **29**, 03A101 (2011); 10.1116/1.3523289

[Hydrogen-related n-type conductivity in hydrothermally grown epitaxial ZnO films](#)

*J. Appl. Phys.* **108**, 083716 (2010); 10.1063/1.3500353

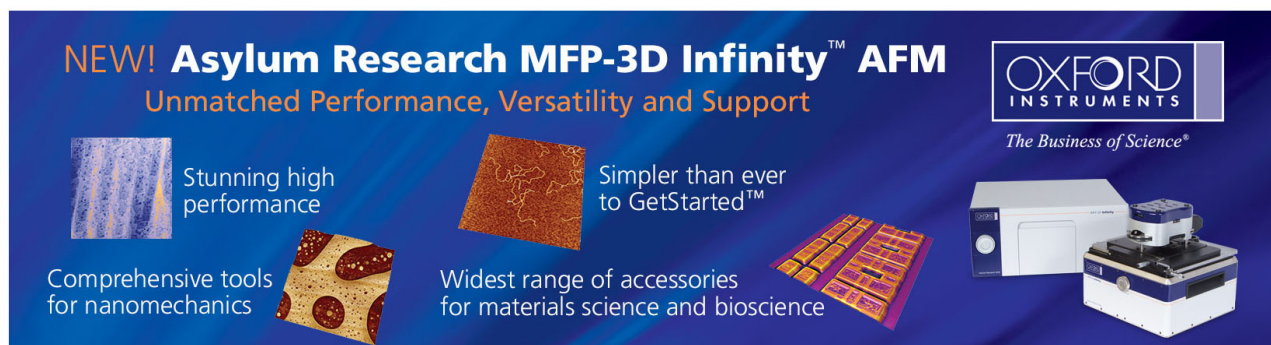
[Structure and interdiffusion of epitaxial ZnO/ZnMgO nanolayered thin films](#)

*J. Vac. Sci. Technol. A* **26**, 1538 (2008); 10.1116/1.2993257

[Study of interfacial diffusion in Al<sub>2</sub>O<sub>3</sub>/ZnO and MgO/ZnO heterostructures](#)

*J. Appl. Phys.* **104**, 016108 (2008); 10.1063/1.2952505

---

This is a promotional banner for the Asylum Research MFP-3D Infinity AFM. The background is dark blue. On the left, the text 'NEW! Asylum Research MFP-3D Infinity™ AFM' is written in white and orange. Below this, the tagline 'Unmatched Performance, Versatility and Support' is in orange. The banner features several images: a 3D surface plot, a microscopic image of a material surface, a collection of AFM accessories, and the physical AFM instrument. Text boxes highlight key features: 'Stunning high performance', 'Simpler than ever to GetStarted™', 'Comprehensive tools for nanomechanics', and 'Widest range of accessories for materials science and bioscience'. The Oxford Instruments logo and the slogan 'The Business of Science®' are in the top right corner.

# Annealing effect on the optical response and interdiffusion of *n*-ZnO/*p*-Si (111) heterojunction grown by atomic layer deposition

Ching-Shun Ku,<sup>1</sup> Jheng-Ming Huang,<sup>2</sup> Ching-Yuan Cheng,<sup>1</sup> Chih-Ming Lin,<sup>3</sup>  
and Hsin-Yi Lee<sup>1,4,a)</sup>

<sup>1</sup>National Synchrotron Radiation Research Center, 101 Hsin-Ann Road, Hsinchu Science Park, Hsinchu 30076, Taiwan

<sup>2</sup>Program for Science and Technology of Accelerator Light Source, National Chiao Tung University, Hsinchu 300, Taiwan

<sup>3</sup>Department of Applied Science, National Hsinchu University of Education, Hsinchu 300, Taiwan

<sup>4</sup>Department of Materials Science and Engineering, National Chiao Tung University, Hsinchu 300, Taiwan

(Received 6 August 2010; accepted 14 October 2010; published online 3 November 2010)

Optical and structural properties of *n*-ZnO films grown on a *p*-Si (111) substrate by atomic layer deposition were observed using *in situ* synchrotron x-ray diffraction during annealing. The photoluminescence showed a complicated photon response with increasing annealing temperature. *In situ* x-ray diffraction indicated the growth of grains for an annealing temperature from 500 to 800 °C with the orientation altering from polycrystalline to preferential (200). Measurements with a time-of-flight secondary-ion mass spectrometer indicated that the outgassing of hydrogen atoms and ZnO/Si interdiffusion behavior were correlated with the intensity and position of emissions in photoluminescence spectra. © 2010 American Institute of Physics. [doi:10.1063/1.3511284]

Having a large direct band gap, 3.37 eV, and a large binding energy, 60 meV, for excitons, ZnO has gained importance for possible applications of these properties,<sup>1</sup> but the small concentration and mobility of holes in *p*-type ZnO layer greatly limit the efficiency of light emission. The fabrication of ZnO-based *p-n* heterojunctions has thus received much attention as an alternative path for optoelectronic applications; *n*-ZnO layers have been deposited on *p*-type materials such as Si, GaN, AlGaN, and SrCu<sub>2</sub>O<sub>2</sub>.<sup>2–8</sup> Among those materials, silicon has prominent merits to make light-emitting diode (LED) devices, because it is not only of interest for the integration of optoelectronic devices but also cheaper than other candidates. Atomic layer deposition (ALD) produces large area films of high quality that are appropriate for industrial application; growth at a low temperature also enables control of the thermodynamics in the process to avoid formation of oxygen vacancies.<sup>9</sup> In the present work, ZnO thin films fabricated at temperature ~25 °C by ALD with interruption of the flow rate (FRI) showed satisfactory near-band-edge (NBE) emission intensity and an insignificant green band.<sup>10</sup> There is no report of the optical response and structural characterization of annealing on the growth of *n*-ZnO/*p*-Si heterojunctions by ALD at a low temperature. Here we present photoluminescence (PL) spectra from a *n*-ZnO/*p*-Si heterojunction measured at 10 K, the origin of compound-related NBE emission bands deduced from *in situ* x-ray diffraction (XRD) and profile results from secondary-ion mass spectrometry (SIMS).

The *n*-ZnO thin film was deposited on a boron-doped *p*-Si (111) substrate at 25 °C with 1000 ALD cycles by a FRI method<sup>10</sup> yielding a film thickness of ~210 nm as determined by measurement of x-ray reflectivity. *In situ* synchrotron XRD with annealing in a range 100–900 °C was performed at wiggler beam-line BL-17B1 in the National

Synchrotron Radiation Research Center (NSRRC), Taiwan; the photon energy was 8 keV with a flux estimated to be 10<sup>11</sup> photons/s. Use of two pairs of slits between the sample and the detector provided a typical wave-vector resolution ~0.001 nm<sup>-1</sup> in the vertical scattering plane in this experiment. For measurements of PL at 10 K, a He-Cd laser (325 nm, IK3252R-E, Kimmon) provided excitation with a UV-enhanced CCD (spec-10, Princeton Instruments, cooled with liquid dinitrogen) after a monochromator (0.5 m, SP2558A, Acton, entrance slit width 10 μm, grating 1200 L/mm, spectral resolution 0.02 nm).

Figure 1 shows the distribution of estimated grain size for varied annealing temperature, deduced from the Scherrer equation,

$$D_{hkl} = \frac{\kappa\lambda}{\beta \cos \theta},$$

in which  $\kappa$  is the shape factor—about 0.89,  $\lambda$  is the x-ray wavelength—1.55 Å in this experiment,  $\beta$  is the full width at

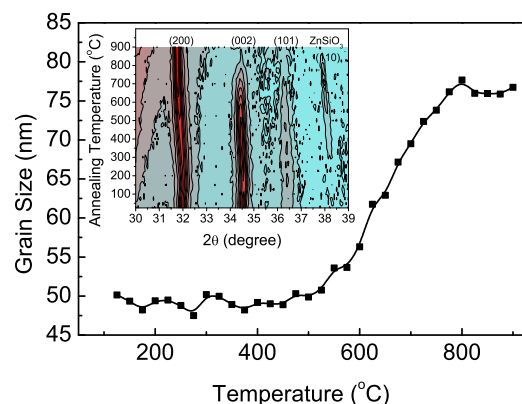


FIG. 1. (Color online) Distribution of grain size with annealing temperature as shown in the figure and inset from *in situ* XRD mapped, which shows a preferred orientation as temperatures greater than 800 °C and a ZnO/Si interface compound formation from 300 to 800 °C.

<sup>a)</sup>Author to whom correspondence should be addressed. Electronic mail: hylee@nsrrc.org.tw.

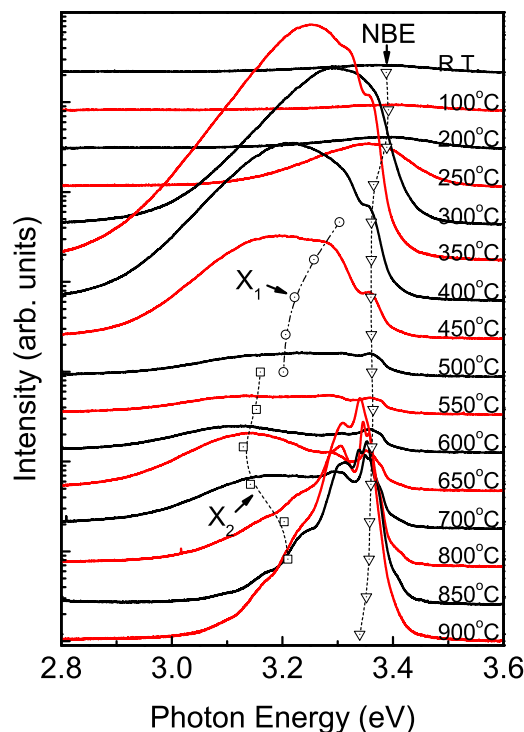


FIG. 2. (Color online) Photoluminescence spectra of  $n$ -ZnO/ $p$ -Si(111) with thermal treatment from 100 to 900 °C. Inset—dashed lines with symbols indicated the positions of lines of NBE, X1 and X2 emission band, respectively.

half maximum (FWHM) in the angular width of the maximum intensity of a diffraction feature ( $hkl$ ),  $\theta$  is the Bragg angle and  $D_{hkl}$  is the grain size or average distance of grain boundary along direction ( $hkl$ ). The grain size remained almost constant for an annealing temperature from 25 to 500 °C, but above 500 °C the grains began to grow and to attain a saturated value of  $\sim 77$  nm at 800 °C. In addition, Bragg peaks (002) and (101) had decreasing intensity with increasing annealing temperature, and disappeared for annealing temperature above 800 °C as shown in the inset of Fig. 1. The orientation of grains in ZnO films altered from random to preferred (200) on annealing at 800 °C, and the intensity of the (200) diffraction signal quadrupled from the value for the sample as grown; these results indicate that crystallites with the  $c$ -axis parallel to the growth direction lie along the sample surface. *In situ* XRD showed an extra feature located at  $2\theta \sim 38^\circ$  that appeared from 300 to 850 °C. According to the results of our XRD refinement, this feature originated from a (110) Bragg peak of zinc silicate,  $\text{ZnSiO}_3$ . The temperature of formation of this  $\text{ZnSiO}_3$  phase was  $\sim 100$  °C less than reported.<sup>11</sup> The low-temperature PL spectra for varied annealing temperature show in Fig. 2 two extra emission lines with labels  $X_1$  and  $X_2$ ; open circles and squares with a dashed line indicate the fitted results of positions from 3.1 eV to 3.3 eV. The temperature distributions of  $X_1$  and  $X_2$  are the same as those of the formation of a  $\text{ZnSiO}_3$  phase shown in XRD patterns (Fig. 1). The NBE position marked with open triangles and a labeled dashed line showed a red-shift behavior for annealing temperatures from 25 to 900 °C. To verify the formation of the  $\text{ZnSiO}_3$  phase at the interface, we grew an amorphous buffer layer of  $\text{Al}_2\text{O}_3$  on Si at 25 °C with 20 ALD cycles yielding a thickness of 2 nm before deposition of the ZnO thin film.

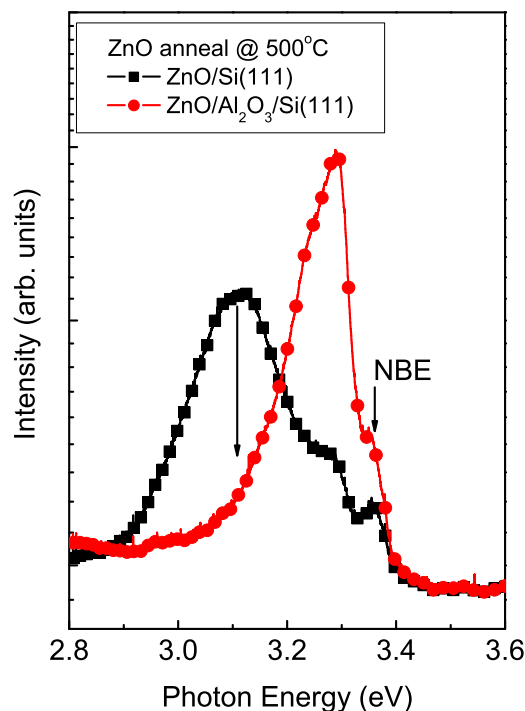


FIG. 3. (Color online) Comparison of photoluminescence spectra of  $n$ -ZnO/ $p$ -Si(111) and  $n$ -ZnO/ $\text{Al}_2\text{O}_3$ / $p$ -Si(111) with a 2 nm  $\text{Al}_2\text{O}_3$  interlayer; the annealing temperature is 500 °C.

Figure 3 show the PL spectra of ZnO thin films with and without the  $\text{Al}_2\text{O}_3$  buffer layer. The feature located at 3.13 eV and related to the  $\text{ZnSiO}_3$  phase vanished with this  $\text{Al}_2\text{O}_3$  buffer layer sample, and the emission band at 3.3 eV called D-band emission was also observed with annealing temperature 850 and 900 °C, shown in Fig. 2, accompanied with two optical-phonon replicas. The existence of such optical-phonon replicas was also reported by Makino *et al.*<sup>12</sup> This feature might be attributed to a piezoelectric, spontaneous polarization effect, or a donor-acceptor pair (DAP) from an alloyed layer. As the Al–O bond energy (511 kJ/mol) is much larger than the Zn–O bond energy (271 kJ/mol) and the Si–O bond energy (452 kJ/mol), it is reasonable to assume that Si–O and Zn–O bonds are much more difficult to break and to react with each other across an  $\text{Al}_2\text{O}_3$  layer. Furthermore, the  $\text{Al}_2\text{O}_3$  buffer layer provided interdiffusion blocking to avoid the recombination path of a non-UV region from the interface, and improved the optical efficiency of Si-based UV devices. Figure 4(a) shows the NBE energy and integrated NBE intensity with varied annealing temperature. The NBE energy decreased from 3.39 to 3.36 eV at 200 °C then increased slightly to 3.365 eV at 550 °C, and finally approached 3.34 eV at 800 °C with increasing annealing temperature. In contrast, the NBE intensity rose and fell as its energy decreased and increased respectively. To understand the behavior of the optical response of a  $n$ -ZnO/ $p$ -Si (111) heterojunction, we applied a secondary-ion mass spectrometer (SIMS) analysis of the distribution of composition of the thin film. The filled squares in Fig. 4(b) show the average intensity of hydrogen concentration of the entire film. The results indicate that the hydrogen intensity decreased  $\sim 80\%$  for temperatures from 200 to 400 °C;  $\sim 18\%$  of hydrogen was recovered at 500 °C. This behavior was observed also on annealing the hydrogen free-carrier absorption in ZnO.<sup>13</sup> The hydrogen concentration showed similar trends with the

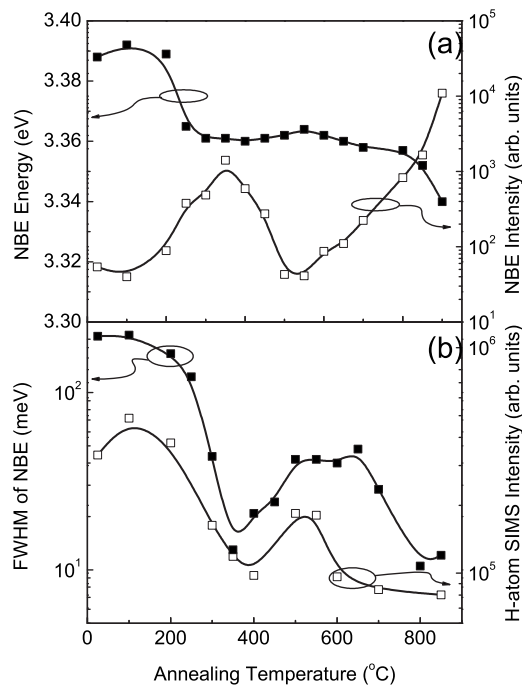


FIG. 4. (a) Filled squares indicate the NBE emission energy and open squares show how the intensity varies with annealing temperature. (b) Filled and open squares show the concentrations of hydrogen and boron atoms, respectively.

NBE energy. The peak position of NBE proved the Burstein–Moss effect.<sup>14</sup> The hydrogen atoms hence act as a shallow donor state in the thin film in agreement with the theoretical work by Van de Walle.<sup>15</sup> The NBE intensity of PL spectra also varied with the hydrogen concentration because of impurity doping that induced a sizable increase of the non-radiative trap center concentration.<sup>16</sup> We observed a broadening of lines on NBE with respect to hydrogen concentration shown in Fig. 4(b); this effect was observed on a heavily doped *n*-type carrier system such as Ga-doped ZnO films.<sup>17</sup> The growth of a thin film of ZnO at 25 °C containing a large concentration of H<sup>+</sup> might result from surface absorption of molecular H<sub>2</sub>O during ALD. In our case, the excess water pulsed into the chamber to ensure the completed reaction between the DEZn precursor and water excludes the possibility of oxygen vacancy. Water is difficult to eliminate from a vacuum system at such a low temperature of growth when the purge gas begins to clear the chamber and the sample surface. A preceding adsorption result<sup>18</sup> indicates that a lower temperature of pretreatment yields more homotactic hydroxylate sites on the ZnO surface, which means that the close-packed surface hydroxyl groups bonded to the ZnO surface result from the formation of mutual hydrogen bonding. We propose that the abundant concentration of the H<sup>+</sup> state via hydroxyl groups remains even after finishing our ALD processes. Also according to DFT calculations,<sup>15</sup> hydrogen is difficult to remove from the crystal matrix. The strong bonds between oxygen and hydrogen atoms also provide a powerful driving force for its incorporation into the ZnO crystal. In this way, there are four possible positions—BC<sub>⊥</sub>, BC<sub>∥</sub>, AB<sub>0,⊥</sub>, and AB<sub>0,∥</sub>, with formation energies  $E^f$  −1.84 eV, −1.82 eV, −1.78 eV, and −1.59 eV,

respectively.<sup>15</sup> The negative formation energy indicates a stable state in the crystal. In our present work,<sup>19</sup> the PL of a ZnO thin film grown on (0002) sapphire near 100 °C also showed greater PL intensity; the reason is that evaporation of surface water at the boiling point decreases the hydrogen contamination in the thin film and enhances the optical emission, although showing a satisfactory crystalline quality at lower temperatures of growth.

In summary, we have presented the effect of annealing on the photoluminescence and structural properties of ZnO films prepared with the ALD technique. We grew a polycrystalline ZnO thin film on Si (111) at 25 °C that showed (200) preferential orientation after thermal annealing over 800 °C; the average grain size grows ~50% from 50 to 77 nm. The NBE intensity of the PL was significantly enhanced by this annealing, and this enhancement correlates with the concentration of residual hydrogen in the ZnO films. An ultrathin Al<sub>2</sub>O<sub>3</sub> layer can serve effectively to block interdiffusion to avoid the X<sub>1</sub> and X<sub>2</sub> emission signals from formation of the ZnSiO<sub>3</sub> phase at the interface. A greater temperature of the substrate or annealing after growth proved an effective way to decrease the concentration of *n*-type free carrier from doped hydrogen and obtain improved quality of PL for the ALD method.

National Science Council of the Republic of China, Taiwan, provided support under Contract Nos. NSC 98-2221-E-213-002, NSC 97-2112-M-134-001-MY2, and NSC 97-2120-M-001-007.

- <sup>1</sup>C. S. Ku, H. Y. Lee, J. M. Huang, and C. M. Lin, *Cryst. Growth Des.* **10**, 1460 (2010).
- <sup>2</sup>H. Paul Maruska, F. Namavar, and N. M. Kalkhoran, *Appl. Phys. Lett.* **61**, 1338 (1992).
- <sup>3</sup>H. Ohta, M. Orita, M. Hirano, and H. Hosono, *J. Appl. Phys.* **89**, 5720 (2001).
- <sup>4</sup>Ya. I. Alivov, J. E. Van Nostrand, D. C. Look, M. V. Chukichev, and B. M. Ataev, *Appl. Phys. Lett.* **83**, 2943 (2003).
- <sup>5</sup>Ya. I. Alivov, E. V. Kalinina, A. E. Cherenkov, D. C. Look, B. M. Ataev, A. K. Omaev, M. V. Chukichev, and D. M. Bagnall, *Appl. Phys. Lett.* **83**, 4719 (2003).
- <sup>6</sup>C. Yuen, S. F. Yu, S. P. Lau, and T. P. Chen, *Appl. Phys. Lett.* **86**, 241111 (2005).
- <sup>7</sup>W. I. Park and G. C. Yi, *Adv. Mater.* **16**, 87 (2004).
- <sup>8</sup>D. C. Look, B. Claflin, Ya. I. Alivov, and S. J. Park, *Phys. Status Solidi A* **201**, 2203 (2004).
- <sup>9</sup>C. G. Van de Walle and R. A. Street, *Phys. Rev. B* **51**, 10615 (1995).
- <sup>10</sup>C. S. Ku, J. M. Huang, C. M. Lin, and H. Y. Lee, *Thin Solid Films* **518**, 1373 (2009).
- <sup>11</sup>X. L. Xu, P. Wang, Z. Qi, H. Ming, J. Xu, H. Liu, C. S. Shi, G. Lu, and W. K. Ge, *J. Phys.: Condens. Matter* **15**, L607 (2003).
- <sup>12</sup>T. Makino, K. Tamura, C. H. Chia, Y. Segawa, M. Kawasaki, A. Ohtomo, and H. Koinuma, *Appl. Phys. Lett.* **81**, 2172 (2002).
- <sup>13</sup>G. A. Shi, M. Stavola, S. J. Pearton, M. Thieme, E. V. Lavrov, and J. Weber, *Phys. Rev. B* **72**, 195211 (2005).
- <sup>14</sup>E. Burstein, *Phys. Rev.* **93**, 632 (1954).
- <sup>15</sup>C. G. Van de Walle, *Phys. Rev. Lett.* **85**, 1012 (2000).
- <sup>16</sup>H. J. Ko, Y. F. Chen, S. K. Hong, H. Wenisch, T. Yao, and D. C. Look, *Appl. Phys. Lett.* **77**, 3761 (2000).
- <sup>17</sup>T. Makino, Y. Segawa, S. Yoshida, A. Tsukazaki, A. Ohtomo, and M. Kawasaki, *Appl. Phys. Lett.* **85**, 759 (2004).
- <sup>18</sup>M. Nagao, *J. Phys. Chem.* **75**, 3822 (1971).
- <sup>19</sup>C. S. Ku, H. Y. Lee, J. M. Huang, and C. M. Lin, *Mater. Chem. Phys.* **120**, 236 (2010).